Cytosolic chaperones influence the fate of a toxin dislocated from the endoplasmic reticulum

Robert A. Spooner[a,1], Philip J. Hart[a], Jonathan P. Cook[a], Paola Pietroni[a], Christian Rogon[b], Jörg Höhfeld[b], Lynne M. Roberts[a], and J. Michael Lord[a]

[a]Department of Biological Sciences, University of Warwick, Coventry CV4 7AL, United Kingdom; and [b]Institut für Zellbiologie, Rheinische Friedrich Wilhelms-Universität Bonn, Ulrich-Haberland-Strasse 61a, 53121 Bonn, Germany

The plant cytotoxin ricin enters target mammalian cells by receptor-mediated endocytosis and undergoes retrograde transport to the endoplasmic reticulum (ER). Here, its catalytic A chain (RTA) is reductively separated from the cell-binding B chain, and free RTA enters the cytosol where it inactivates ribosomes. Cytosolic entry requires unfolding of RTA and dislocation across the ER membrane such that it arrives in the cytosol in a vulnerable, nonnative conformation. Clearly, for such a dislocated toxin to become active, it must avoid degradation and fold to a catalytic conformation. Here, we show that, *in vitro*, Hsc70 prevents aggregation of heat-treated RTA, and that RTA catalytic activity is recovered after chaperone treatment. A combination of pharmacological inhibition and cochaperone expression reveals that, *in vivo*, cytosolic RTA is scrutinized sequentially by the Hsc70 and Hsp90 cytosolic chaperone machineries, and that its eventual fate is determined by the balance of activities of cochaperones that regulate Hsc70 and Hsp90 functions. Cytotoxic activity follows Hsc70-mediated escape of RTA from an otherwise destructive pathway facilitated by Hsp90. We demonstrate a role for cytosolic chaperones, proteins typically associated with folding nascent proteins, assembling multimolecular protein complexes and degrading cytosolic and stalled, cotranslocational clients, in a toxin triage, in which both toxin folding and degradation are initiated from chaperone-bound states.

Hsc70 | Hsp90 | ricin

Endoplasmic-reticulum (ER) associated protein degradation (ERAD) comprises coordinated disposal systems that recognize and remove misfolded and unassembled proteins in the ER, dislocating them across the ER membrane to the cytosol for proteasomal destruction. Degradation is normally facilitated by polyubiquitylation, usually on internal lysyl residues of the target protein. Both membrane-bound and soluble ER proteins can be disposed of by ERAD (1, 2).

The plant cytotoxin ricin traffics to the ER lumen of mammalian cells where it is reduced to its RTA and RTB subunits before RTA dislocation (3). RTA does not penetrate the ER membrane directly; instead it exploits pre-existing protein-conducting channels as a nonnative species, mimicking ER proteins dispatched via ERAD (4, 5). Thus, it enters the cytosol in a form susceptible to proteolysis or aggregation. A proportion must evade these fates to gain a catalytic conformation that depurinates target ribosomes, stopping protein synthesis. The paucity of lysine residues in RTA may facilitate uncoupling from ERAD by reducing the potential for polyubiquitylation, thereby hampering proteasomal degradation (6). This, in turn, may provide opportunities for spontaneous or chaperone-assisted folding not normally sanctioned for ERAD substrates.

We show an interaction of RTA with the cytosolic heat shock (cognate) protein Hsc70. From the chaperone-bound state, nonnative cytosolic RTA can achieve a catalytic conformation or can be inactivated. Its ultimate fate depends on the activities of cochaperones that regulate Hsc70.

Results

Inhibition of Hsc70 Protects HeLa Cells from Ricin.
Ricin binds exposed galactosyl residues, opportunistically exploiting a huge number of surface glycoproteins (3). Consequently, trafficking pathways are diverse with <5% of the cell-surface bound toxin reaching the TGN (7). Of this, only a tiny proportion reaches the ER (8) and subsequently the cytosol. RTA is not modified in transit, so the toxic cytosolic fraction cannot be distinguished from the overwhelming noncytotoxic majority at the cell surface and in the endomembrane system by immunoblotting, cellular fractionation, indirect immunofluorescence, or coimmunoprecipitation approaches. However, ricin cytotoxicity correlates strongly with ribosome depurination, so it can be used as a measure of the relative amount of native RTA in the cytosol (9).

Deoxyspergualin (DSG) alters the ATPase activity of the cytosolic heat-shock (cognate) protein Hsc70 *in vitro*, and *in vivo* permits expression of functional cystic fibrosis transmembrane conductance regulator (CFTR) in cells expressing mutant ΔF508CFTR, presumably by inhibiting interactions with Hsc70 chaperone complexes that target it to proteasomes (10, 11). When DSG was added with ricin to HeLa cells, the cells became ~3-fold more resistant to toxin (Fig. 1 *A* and *B*), suggesting that an increased proportion of toxin remained inactive. DSG alone had no effect on protein synthesis (Fig. 1*C*). The ER Hsp70 counterpart BiP is not affected by DSG (12), suggesting that protection occurred in the cytosol. After ricin challenge, a distinct lag before the onset of cytotoxicity that represents trafficking time from cell surface to the first destruction of ribosomes (13) is unchanged by DSG treatment (Table 1), confirming that the effect of DSG occurs in the cytosol, and not by interfering with toxin delivery. Because unfolding is necessary to render RTA competent for dislocation (5), then folding must be required for catalytic activity in the cytosol, and this appears to involve Hsc70. In contrast, DSG had no effect on the potency of diphtheria toxin (DTx, Fig. 1 *A* and *B*), which enters the cytosol from acidified endosomes, refolding spontaneously in the cytosol (14).

Inhibition of Hsp90 Sensitizes Cells to Ricin.
DSG also interacts with the cytosolic chaperone Hsp90 (10). To clarify its most upstream target, we used geldanamycin (GA) and radicicol (RA), competitive inhibitors of the Hsp90 ATP-binding site (15). Treatment with 1 μM GA or RA resulted in a ~1.5- to 2-fold sensitization of cells to ricin (Fig. 2 *A* and *B*), without altering toxin trafficking times (Table 1). Treatments with GA or RA alone have little, if any, effect on protein synthesis (Fig. 2*C*).

Fig. 1. Deoxyspergualin (DSG) protects HeLa cells from ricin intoxication. (*A*) Cells were treated for 4 h with graded doses of ricin or diphtheria toxin (DTx) in growth medium containing 50 μg ml^{-1} DSG/100 μg ml^{-1} lactose (filled circles) or 100 μg ml^{-1} lactose carrier only (open circles), and their subsequent ability to synthesize proteins was determined by measuring incorporation of [^{35}S]-Met into acid-precipitable material. Typical single assays are shown. (*B*) Control cells and cells pretreated (pre) with DSG/lactose were treated as in *A*, sensitivities to toxin (IC$_{50}$, toxin concentration required to reduce protein synthesis to 50% that of nontoxin treated controls) were determined, and fold protection (IC$_{50}$ DSG-treated cells: IC$_{50}$ control cells) is displayed. Means of three (DTx, ricin 16-h DSG pretreatment) or six (ricin, no DSG pretreatment) independent experiments are displayed. (Bars, $\pm$1 S.D.; broken line, no protective effect over that of treatment with lactose carrier only). (*C*) Cells were treated with lactose (lac) or lactose/DSG only as appropriate for 4 h, and remaining protein synthesis ability was determined. (*n* = 3; bars, $\pm$1 S.D.)

Prolonged inhibition of Hsp90 by GA up-regulates Hsp72 (16). We saw the same, confirming activity of GA and RA under our conditions (Fig. 2*D*). Our sensitizing effects were obtained by using acute drug treatments, before up-regulation of Hsp72, but even with a 4-h drug pretreatment, cells were still sensitized to ricin (data not shown). Thus, the effects of GA and RA do not arise through augmented levels of Hsp72. GA and RA also interact with GRP94, the ER counterpart of Hsp90. NECA (N-ethylcarboxamidoadenosine), a GRP94 inhibitor that does not affect Hsp90 (17) protected cells slightly from ricin (1.48 $\pm$ 0.34 -fold, *n* = 5), confirming that the sensitizing effects of GA and RA arose from inhibition of cytosolic Hsp90 and not GRP94 (Fig. 2*B*). It also suggests a role for GRP94 in preparing RTA for dislocation, consistent with its ability to direct the null Hong Kong variant of α1-antitrypsin to ERAD (18).

These data suggest that the fate of RTA is determined by cytosolic triage, with an activation arm (toxin-sensitizing) inhibited by DSG and an inactivation arm (protective) inhibited by GA and RA. Combined treatment with DSG and RA gave a net protective effect against ricin (Fig. 2*B*), demonstrating a sequential process with the step promoted by Hsc70 lying upstream of the step mediated by Hsp90.

Hsc70 Interacts with RTA *in Vitro*. Because the minuscule amounts of cytosolic RTA preclude detection except by monitoring the consequences of its catalytic action, interactions with Hsp70 and its cochaperone Hsp40 were examined *in vitro*. Brief heating to 45°C destabilizes RTA structure (19). RTA became insoluble (P, pellet) after such treatment (15 min), with ~10% remaining soluble (S) after centrifugation (Fig. 3*A*, upper panel, upper graph). Incremental increases in recovery of soluble material were obtained by adding Hsp40, Hsp70, or both before heating. Maximal chaperone-mediated solubility required ATP. These

data suggest that a potential role for these chaperones *in vivo* could be to prevent vulnerable dislocated RTA from aggregating. Hsp40 was insoluble after heat treatment, alleviated by addition of Hsc70. Repeating these assays in the absence of RTA showed that this is its normal behavior (Fig. 3*A*, middle panel).

Fig. 2. Geldanamycin (GA) and radicicol (RA) sensitize HeLa cells to ricin challenge. (*A*) Cells were treated (4 h) with increasing doses of ricin in medium containing GA/DMSO (black circles), RA/DMSO (gray circles), or DMSO vehicle only (white circles), and their subsequent ability to synthesize proteins was determined as in Fig. 1*A*. Typical single assays are shown. (*B*) Cells were challenged as in (*A*), IC$_{50}$ values were determined as in Fig. 1*B*, and the effects of GA and RA are displayed as fold sensitizations (IC$_{50}$ GA- or RA-treated cells: IC$_{50}$ control DMSO-treated cells). Also shown are the effects of treatment with NECA, and combined treatments with RA, DSG, and DMSO. Means of three independent experiments are displayed, except for NECA treatment, where *n* = 5. (Bars, $\pm$1 S.D.; broken line, no effect over that of treatment with DMSO vehicle only) (*C*) Cells were treated with vehicle DMSO, DMSO/GA, or DMSO/RA as appropriate for 4 h, and remaining protein synthesis ability was determined. (*n* = 3; bars, $\pm$1 S.D.) (*D*) Immunoblots of detergent soluble cell extracts (25 μg protein per lane) from cells incubated for various lengths of time (t) in growth medium containing 1 μM GA or 1 μM RA were probed for Hsp72 (upper strip), Hsp90 (middle strip), or γ-tubulin (lower strip).

Table 1. Ricin cell-surface to cytosol trafficking times

Treatment	T, min
100 μg ml^{-1} lactose carrier	62.4 $\pm$ 1.2
50 μg ml^{-1} DSG/ lactose	64.7 $\pm$ 1.8
0.001% DMSO vehicle	68.0 $\pm$ 6.3
1 μM geldanamycin/DMSO	63.4 $\pm$ 9.8
1 μM radicicol/DMSO	65.2 $\pm$ 8.3

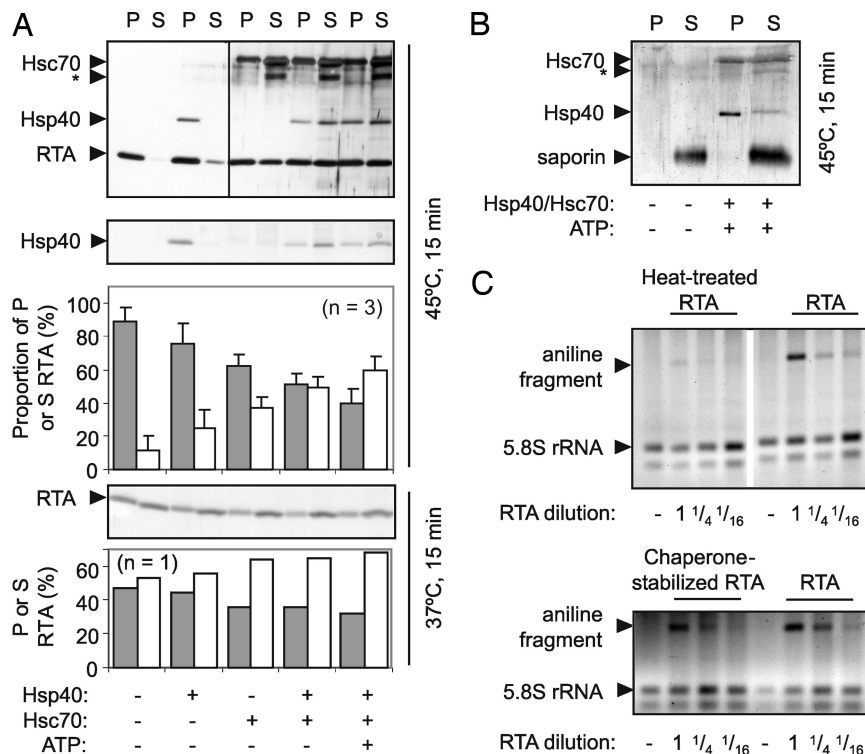T, *n* = 3–6, $\pm$ 1 SD.

CELL BIOLOGY

Fig. 3. *In vitro* interactions of RTA and Hsp40 and Hsc70 chaperones. (*A*) RTA (500 ng) was incubated at the indicated temperatures for 15 min in 20 μl of 20 mM Mops pH 7.2, 100 mM KCl, in the presence or absence of Hsp40, Hsc70, or ATP (shown below the panels). Aggregated (P) and soluble (S) fractions were separated by centrifugation, heated in reducing SDS sample buffer, and analyzed by SDS/PAGE and subsequent silver staining. *, proteolytic fragment of Hsc70 lacking the C-terminal regulatory domain. Proportions (%) of aggregated (gray) and soluble (white) RTA are shown. (Bars, ±1 S.D.) (*B*) Reaction mixtures where RTA was replaced by saporin were treated as in (*A*). (*C*) Dilutions of the soluble fractions from 375 ng of heat-treated RTA (upper panel), 375 ng of chaperone-stabilized RTA (lower panel), and 375 ng of native RTA were added to yeast ribosomes for 2 h at 30°C. After cleavage of any depurinated 28S rRNA with acetic-aniline, rRNAs were extracted, electrophoresed in denaturing conditions (1.2% agarose, 50% formamide), and gels were stained with ethidium bromide before quantifying (22).

When RTA was heated for 15 min with or without chaperones at 37°C, the chaperones had a similar although less pronounced effect (Fig. 3*A*, lower panel, lower graph). Saporin has a largely indistinguishable tertiary structure relative to RTA with identical, superimposable active site residues and has identical activity against ribosomes (20), but it lacks the C-terminal hydrophobic stretch that in RTA has been implicated in membrane interactions preceding dislocation (21). Saporin showed no thermal instability (Fig. 3*B*) after heating at 45°C. This result contrasts with the instability of RTA and its recognition by Hsp40/Hsc70 even at 37°C, and suggests that interactions with Hsc70 might be a normal feature of folded RTA in the cytosol.

To investigate whether chaperone-treated RTA had catalytic activity, dilutions of the soluble fractions from heat-treated RTA and chaperone-stabilized RTA were added to yeast ribosomes, which were subsequently treated with acidified aniline. Correctly folded RTA specifically depurinates yeast 26S rRNA, and aniline treatment cleaves the phosphodiester bond at the depurination site, releasing a small diagnostic fragment of RNA (22). As expected, a small amount of RTA activity remained after heat-treatment, but almost full activity was recovered from chaperone-stabilized RTA (Fig. 3*C*). We conclude that the major proportion of denatured RTA with chaperone-mediated solubility is, or can become, competent to gain catalytic activity.

Hsc70 Cochaperone Activity Determines the Fate of Dislocated RTA *in Vivo*. Having established that RTA interacts with Hsc70 *in vitro* and that catalytic activity can be recovered from the chaperone-

bound state, we examined the effects of modulating Hsc70 cochaperone activities *in vivo*.

The dual cochaperone Hsc70-Hsp90 organizing protein (Hop) recruits Hsp90 to pre-existing Hsc70-client complexes, transferring client proteins from Hsc70 to Hsp90 (23). Transient overexpression of Hop protected cells from ricin challenge (Fig. 4 *A* and *C*), suggesting that increased links between Hsc70 and Hsp90 lead to increased toxin turnover, consistent with the sensitizing effects of GA/RA that block entry into the Hsp90 cycle. Thus, sequential interaction with Hsc70 and Hsp90 directs cytosolic RTA toward net inactivation.

BCL2-associated athanogene protein (BAG-1) isoforms are nucleotide exchange factors that stimulate release of Hsc70-bound clients and bear a ubiquitin-like (ubl) motif that interacts with the proteasome (24). Transient overexpression of BAG-1 protected cells against ricin (Fig. 4 *B* and *D*). Thus, BAG-1 may stimulate release of Hsc70-bound RTA on a path toward inactivation, consistent with the increased sensitivity of cells to ricin reported after inhibition of proteasome activity (25).

Both Hsc70- and Hsp90- complexes can become sorting machines that promote client destruction. C terminus of Hsp70-interacting protein (CHIP) is an E3 ubiquitin ligase that interacts with Hsc70 and Hsp90, and with its partner ubiquitin-conjugating enzymes initiates proteasomal sorting by ubiquitylating chaperone-bound substrates. Transient over-expression of CHIP resulted in enhanced inactivation of RTA, seen as increased resistance of cells to ricin (Fig. 4 *B* and *E*).

To investigate whether Hsc70 can also promote toxin activity *in vivo*, we overexpressed Hsp70-interacting protein (Hip), a Hsc70 cochaperone, which stabilizes ADP-bound Hsc70, in-

Fig. 4. Hsc70 cochaperone activity determines the fate of dislocated RTA *in vivo*. (*A*) Cells transiently transfected with an expression plasmid expressing Hop (Hop/Hop), with an equimolar mixture of plasmids expressing LacZ and Hop (Hop/LacZ), or with a plasmid expressing LacZ (LacZ/LacZ) were assayed for ricin sensitivity. Values were corrected for transfection efficiency, determined as 35% by epifluorescent examination of cells transiently transfected with a plasmid expressing GFP. Dotted line, no effect over that of LacZ transfection. (*B*) Cells were transfected, as in (*A*), with expression plasmids expressing LacZ, BAG-1S [the small (S) isomer of BAG-1], CHIP, Hip, or BAG-2 and were assayed for ricin sensitivity compared with cells transfected coevally with vector alone. Dotted line, no protective effect over vector transfection. (*C–G*) Interactions of cochaperones with Hsc70 and client protein (red line).

creasing client residence and presumably permitting greater opportunity for productive folding (26). Over-expression of Hip-sensitized cells to ricin challenge (Fig. 4 *B* and *F*); thus, Hip controls an activation arm of RTA triage.

The BAG-2 nucleotide exchange factor lacks the ubl domain of BAG-1 and thus, cannot link a client:chaperone complex directly to the proteasome. It also inhibits CHIP activity (27). These properties allow it to facilitate maturation of newly synthesized CFTR, diverting the receptor from the proteasome pathway (28). Consistent with this, BAG-2 overexpression increased the sensitivity of cells to ricin (Fig. 4 *B* and *G*), demonstrating diversion of RTA from a destructive fate. We conclude that the ultimate fate of cytosolic RTA is determined by the relative expression levels of Hsc70 cochaperones.

RTA Can Be a Substrate for CHIP. Our inhibitor and expression data demonstrate that activation and inactivation arms for RTA proceed from Hsc70, and suggest that inactivation may require a ubiquitin signal, either indirectly [via the interlaced ubl domain of BAG-1 or perhaps in a piggy-back mechanism through Hsc70 ubiquitylation (29)], or directly (as CHIP-mediated RTA ubiquitylation). To examine the latter, purified RTA was added to reaction mixtures in which CHIP activity can be recapitulated *in vitro* (30), which were then incubated for 2 h at 30°C. In complete reaction mixtures and also when E1 (ubiquitin activating enzyme), E2 (ubiquitin conjugating enzyme), CHIP, or Hsp40/Hsc70 were individually absent from the reconstitutions, no ubiquitylation of RTA was seen (data not shown). However, after mild thermal denaturation (45°C, 10 min) followed by

incubation at 30°C in complete reaction mixture not only was Hsc70 ubiquitylated (Fig. 5*A*, Ub-Hsc70, upper panel) but so was a small proportion of RTA (Fig. 5*A*, Ub-RTA, lower panel). An even smaller proportion of RTA was a substrate for isolated CHIP.

The scrutiny of native RTA at 37°C by Hsc70 complexes that was noted previously (Fig. 3*A*) was also seen with Hsc70/CHIP complexes. After incubation at 37°C for 2 h in the absence of E1, there was no ubiquitylation of Hsc70, CHIP, or RTA (Fig. 5*B*). Upon addition of E1, both Hsc70 and CHIP became ubiquitylated, events that occur *in vivo* that reflect regulation of Hsc70 by CHIP (28). Not all proteins are ubiquitylated in these conditions, for example, BAG-2 inhibits CHIP activity without becoming ubiquitylated (28). A recombinant version of RTA containing four extra lysyl residues (RTA 6K) was more heavily ubiquitylated under these conditions, consistent with its enhanced propensity for proteasomal degradation (25). A small proportion of native wild-type RTA (2K) was also a substrate for the Hsc70/CHIP cochaperone machinery (Fig. 5*B*).

Hsp90 also prevented aggregation of heat-treated RTA *in vitro*, but in an ATP-independent manner (Fig. 5*C*, upper panel and graph), but, unlike Hsc70, had no effect at 37°C (Fig. 5*C*, lower panel and graph). Furthermore, in *in vitro* CHIP-mediated ubiquitylation assays at 37°C, Hsp90 alone could not direct CHIP efficiently toward RTA, but in the presence of Hsc70 and HOP, Hsp90 promoted RTA ubiquitylation, thus providing a rationale for the net protective effect of Hsp90 *in vivo* (Fig. 5*D*). We conclude that both nonnative and native RTA at the physiological temperature for ricin intoxication can be substrates for Hsc70- and Hsp90-CHIP complexes, and that sequential Hsc70-Hsp90 interactions lead to net RTA inactivation.

Discussion

Molecular chaperones are widely regarded as cellular protein folding factors governing folding of nascent and damaged protein clients, and as protein assembly factors. During ER translocation, yeast cytosolic chaperones target ER import-incompetent proteins to the proteasome (31). In mammalian cells, roles for Hsc70 have been demonstrated in CFTR triage (32) and in cotranslocational destruction of apoB that has stalled in the import translocon (33). Here, we demonstrate that a luminal protein that exploits the ERAD pathway for dislocation is also scrutinized by the same machineries. Prevailing concentrations of Hsc70 cochaperones determine the proportion of toxin that can recover catalytic activity and the proportion that is destroyed. The simplest model to account for our findings is shown in Fig. 5*E*, illustrating chaperone-mediated triage of cytosolic RTA. After dislocation, RTA is recognized by the Hsc70 chaperone machinery. Cochaperones BAG-2 and Hip promote RTA activity *in vivo*, resulting in increased sensitivity of cells to ricin. Inactivation arms also proceed from Hsc70, controlled by BAG-1 and CHIP, protecting the cell from ricin toxicity. In addition, the dual cochaperone Hop coordinates a sequential Hsc70-Hsp90 triage whose net effect is to render dislocated RTA inactive. Inactivation may be mediated by ubiquitylation machineries. Both gain of catalytic conformation and degradation of RTA proceed from chaperone-bound states. This is highly reminiscent of the Hsc70-Hsp90 mediated regulation of signaling proteins (34), but may be unprecedented for a soluble protein that is dislocated from the ER lumen, because soluble ERAD substrates typically interact with other membrane-associated chaperone machineries (35), whereas cytosolic domains of misfolded membrane proteins typically interact with Hsc70 complexes (36). Our findings emphasize the central role of Hsc70-Hsp90 chaperone machineries in cytosolic protein triage. A minimal role for Hsc70 appears to be to prevent aggregation of dislocated RTA in the cytosol, but the possibility
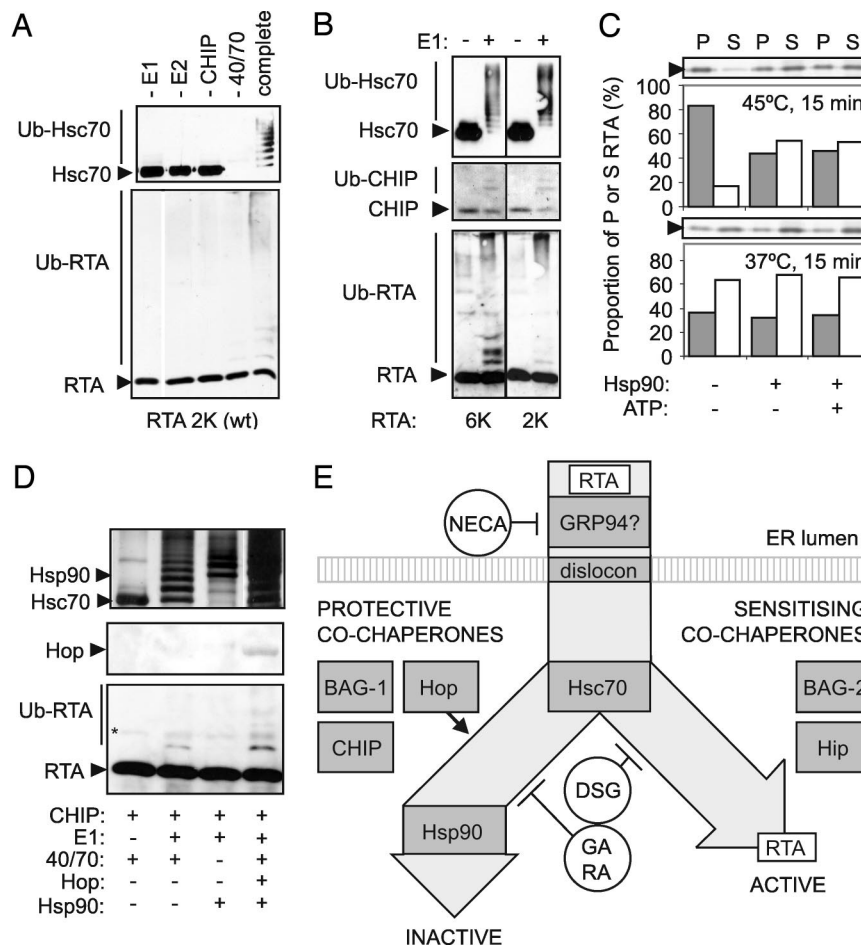
Fig. 5. RTA is a substrate for CHIP. (*A*) RTA was added to a reaction mixture (complete), which can recapitulate CHIP activity (28), and to mixtures lacking E1 ubiquitin activating enzyme, E2 (UbcH5 ubiquitin conjugating enzyme), CHIP, or Hsp40/Hsc70 (40/70) as indicated. After heating (45°C, 10 min), reactions were activated by addition of 5 mM MgCl₂, 10 mM DTT, and 5 mM ATP, incubated (2h, 30°C), and products were identified by reducing SDS/PAGE and immunoblotting for Hsc70 and RTA. (*B*) Addition of E1 to a reaction mixture containing RTA, Hsp40, Hsc70, E2, CHIP, and ubiquitin as in *A*, and incubation at 37°C for 2 h results in CHIP-mediated ubiquitylation of Hsc70 (upper panel, Ub-Hsc70), CHIP (middle panel, Ub-CHIP), and both RTA 6K and RTA (lower panel, Ub-RTA) as revealed by immunoblots. (*C*) RTA (500 ng) was incubated (45°C or 37°C, 15 min) in the presence or absence of Hsp90 or ATP (shown below the panels). Aggregated (P) and soluble (S) fractions were separated by centrifugation, heated in reducing SDS sample buffer, and analyzed by SDS/PAGE and subsequent silver staining. Proportions (%) of aggregated (gray) and soluble (white) RTA are shown. (*D*) RTA was added to CHIP recapitulation mixtures as in *A*, but containing Hsp40 and Hsp70 (40/70), HOP, and Hsp90 as indicated below the panels, incubated (2 h, 37°C), and products were identified by reducing SDS/PAGE and immunoblotting for HOP and RTA, and by silver staining for Hsc70 and Hsp90. ∗, cross-reacting contaminant. (*E*) Proposed cytosolic triage of dislocated RTA.

of Hsc70 supporting the folding of RTA directly cannot yet be discounted.

Folding of heat-denatured RTA *in vitro* is favored in the presence of ribosomes, implicating the toxin's substrate in its own activation (19). It remains to be seen whether human homologues of ribosome-tethered chaperones that assist folding of nascent proteins (37, 38) also contribute to posttranslational folding of cytosolic RTA and how significant a role they have relative to the soluble chaperone complexes.

Materials and Methods

Cytotoxicity Measurements. HeLa cell responses to 4-h challenges with graded doses of ricin or diphtheria toxin (DTx) were measured as previously described (3). For pharmacological studies, cells were treated coevally with graded doses of toxin in medium containing carrier or solvent vehicle (control) and with toxin dilutions in medium containing both carrier/vehicle and pharmacological agent. Each cytotoxicity curve was normalized to controls not treated with toxin, but containing agent or vehicle as appropriate, so any effects of agent alone on protein synthesis were accounted for. Toxin trafficking times from cell surface to first destruction of ribosomes were measured as previously described (13). DSG was supplied by Worldwide Clinical Development, Nippon Kayaku Co., Ltd., 31–12, Shimo 3-chome, Kita-ku, Tokyo 115-0042, Japan.

Overexpression Studies. HeLa cells were transfected with vectors expressing cochaperones, using previously published conditions (3). Two days posttransfection, cells were seeded into 96-well plates and grown overnight for cytotoxicity studies. Overexpression of cochaperones was confirmed by using FLAG-tagged versions of these proteins, and immunoblotting using an anti-FLAG antibody (data not shown).

***In Vitro* Ubiquitylation, Aggregation, and RTA Activity Studies.** Recombinant RTA was added to reaction mixtures containing 0.1 μM E1 ubiquitin activating enzyme, 0.3 μM Hsp40, 3 μM Hsc70, 3 μM HOP, 3 μM Hsp90, 4 μM UbcH5 (E2 conjugating enzyme), 3 μM CHIP, and 2 mg.ml⁻¹ ubiquitin in 20 mM Mops, pH 7.2, 100 mM KCl, 5 mM MgCl₂, 5 mM ATP, 10 mM DTT buffer as previously described (28) and to reaction mixtures lacking components as appropriate. After incubation (2 h) at 30°C or 37°C as appropriate, products were identified by reducing SDS/PAGE and immunoblot. When required, reaction mixes lacking ATP and MgCl₂ were heated to 45°C for 10 min followed by cooling to the required reaction temperature and activation of the reaction by addition of ATP and MgCl₂. For aggregation studies, reaction mixtures lacking E1, E2, CHIP, and Ub were used, and RTA was heated to 37°C or 45°C in the presence or absence of Hsp40, Hsc70, Hsp90, and ATP. Aggregated and soluble fractions were separated by centrifugation (16,000 × *g*, 10 min), solubilized in reducing SDS sample buffer, and analyzed by SDS/PAGE and silver staining. Catalytic activity of RTA from soluble fractions was assayed by quantifiying the RNA

fragment released from yeast 26S rRNA after RTA-mediated depurination of intact ribosomes and cleavage with acetic-aniline. rRNA species were resolved by denaturing gel electrophoresis, and fragments quantified in relation to the amount of 5.8S rRNA (22). Bands on silver-stained and ethidium bromide stained gels were quantified by using TotalLab software.

1. Brodsky JL (2007) The protective and destructive roles played by molecular chaperones during ERAD (endoplasmic-reticulum-associated degradation). *Biochem J* 404:353–363.
2. Meusser B, Hirsch C, Jarosch E, Sommer T (2005) ERAD: The long road to destruction. *Nat Cell Biol* 7:766–772.
3. Spooner RA, *et al.* (2004) Protein disulfide-isomerase reduces ricin to its A and B chains in the endoplasmic reticulum. *Biochem J* 383:285–293.
4. Wesche J, Rapak A, Olsnes S (1999) Dependence of ricin toxicity on translocation of the toxin A-chain from the endoplasmic reticulum to the cytosol. *J Biol Chem* 274:34443–34449.
5. Argent RH, *et al.* (1994) Introduction of a disulfide bond into ricin A chain decreases the cytotoxicity of the ricin holotoxin. *J Biol Chem* 269:26705–26710.
6. Hazes B, Read RJ (1997) Accumulating evidence suggests that several AB-toxins subvert the endoplasmic reticulum-associated protein degradation pathway to enter target cells. *Biochemistry* 36:11051–11054.
7. van Deurs B, *et al.* (1988) Estimation of the amount of internalized ricin that reaches the trans-Golgi network. *J Cell Biol* 106:253–267.
8. Rapak A, Falnes PO, Olsnes S (1997) Retrograde transport of mutant ricin to the endoplasmic reticulum with subsequent translocation to cytosol. *Proc Natl Acad Sci USA* 94:3783–3788.
9. Wales R, Roberts LM, Lord JM (1993) Addition of an endoplasmic reticulum retrieval sequence to ricin A chain significantly increases its cytotoxicity to mammalian cells. *J Biol Chem* 268:23986–23990.
10. Nadeau K, *et al.* (1994) Quantitation of the interaction of the immunosuppressant deoxyspergualin and analogs with Hsc70 and Hsp90. *Biochemistry* 33:2561–2567.
11. Meacham GC, *et al.* (2001) The Hsc70 co-chaperone CHIP targets immature CFTR for proteasomal degradation. *Nat Cell Biol* 3:100–105.
12. Brodsky JL (1999) Selectivity of the molecular chaperone-specific immunosuppressive agent 15-deoxyspergualin: Modulation of Hsc70 ATPase activity without compromising DnaJ chaperone interactions. *Biochem Pharmacol* 57:877–880.
13. Hudson TH, Neville DM, Jr (1987) Temporal separation of protein toxin translocation from processing events. *J Biol Chem* 262:16484–16494.
14. Ramsay G, Montgomery D, Berger D, Freire E (1989) Energetics of diphtheria toxin membrane insertion and translocation: Calorimetric characterization of the acid pH induced transition. *Biochemistry* 28:529–533.
15. Roe SM, *et al.* (1999) Structural basis for inhibition of the Hsp90 molecular chaperone by the antitumor antibiotics radicicol and geldanamycin. *J Med Chem* 42:260–266.
16. Lawson B, Brewer JW, Hendershot LM (1998) Geldanamycin, an hsp90/GRP94-binding drug, induces increased transcription of endoplasmic reticulum (ER) chaperones via the ER stress pathway. *J Cell Physiol* 174:170–178.
17. Rosser MF, Nicchitta CV (2000) Ligand interactions in the adenosine nucleotide-binding domain of the Hsp90 chaperone, GRP94 I: Evidence for allosteric regulation of ligand binding. J Biol Chem 275:22798–22805.
18. Christianson JC, Shaler TA, Tyler RE, Kopito RR (2008) OS-9 and GRP94 deliver mutant alpha1-antitrypsin to the Hrd1-SEL1L ubiquitin ligase complex for ERAD. *Nat Cell Biol* 10:272–282.
19. Argent R H, *et al.* (2000) Ribosome-mediated folding of partially unfolded ricin A-chain. *J Biol Chem* 275:9263–9269.
20. Savino C, *et al.* (2000) The crystal structure of saporin SO6 from Saponaria officinalis and its interaction with the ribosome. *FEBS Lett* 470:239–243.
21. Day PJ, Pinheiro TJ, Roberts LM, Lord JM (2002) Binding of ricin A-chain to negatively charged phospholipid vesicles leads to protein structural changes and destabilizes the lipid bilayer. *Biochemistry* 41:2836–2843.
22. Chaddock JA, Roberts LM (1993) Mutagenesis and kinetic analysis of the active site Glu177 of ricin A-chain. *Protein Eng* 6:425–431.
23. Chen S, Smith DF (1998) Hop as an adaptor in the heat shock protein 70 (Hsp70) and hsp90 chaperone machinery. *J Biol Chem* 273:35194–35200.
24. Luders J, Demand J, Hohfeld J (2000) The ubiquitin-related BAG-1 provides a link between the molecular chaperones Hsc70/Hsp70 and the proteasome. *J Biol Chem* 275:4613–4617.
25. Deeks ED, *et al.* (2002) The low lysine content of ricin A chain reduces the risk of proteolytic degradation after translocation from the endoplasmic reticulum to the cytosol. *Biochemistry* 41:3405–3413.
26. Hohfeld J, Minami Y, Hartl FU (1995) Hip, a novel cochaperone involved in the eukaryotic Hsc70/Hsp40 reaction cycle. *Cell* 83:589–598.
27. Dai Q, *et al.* (2005) Regulation of the cytoplasmic quality control protein degradation pathway by BAG2. *J Biol Chem* 280:38673–38681.
28. Arndt V, *et al.* (2005) BAG-2 acts as an inhibitor of the chaperone-associated ubiquitin ligase CHIP. *Mol Biol Cell* 16:5891–5900.
29. Urushitani M, *et al.* (2004) CHIP promotes proteasomal degradation of familial ALS-linked mutant SOD1 by ubiquitinating Hsp/Hsc70. *J Neurochem* 90:231–244.
30. Jiang J, *et al.* (2001) CHIP is a U-box-dependent E3 ubiquitin ligase: Identification of Hsc70 as a target for ubiquitylation. *J Biol Chem* 276:42938–42944.
31. Park SH, *et al.* (2007) The cytoplasmic Hsp70 chaperone machinery subjects misfolded and endoplasmic reticulum import-incompetent proteins to degradation via the ubiquitin-proteasome system. *Mol Biol Cell* 18:153–165.
32. Younger JM, *et al.* (2006) Sequential quality-control checkpoints triage misfolded cystic fibrosis transmembrane conductance regulator. *Cell* 126:571–582.
33. Gusarova V, Caplan AJ, Brodsky JL, Fisher EA (2001) Apoprotein B degradation is promoted by the molecular chaperones hsp90 and hsp70. *J Biol Chem* 276:24891–24900.
34. Arndt V, Rogon C, Hohfeld J (2007) To be, or not to be–molecular chaperones in protein degradation. *Cell Mol Life Sci* 64:2525–2541.
35. Nakatsukasa K, Brodsky JL (2008) The recognition and retrotranslocation of misfolded proteins from the endoplasmic reticulum. *Traffic* 9:861–870.
36. Nakatsukasa K, Huyer G, Michaelis S, Brodsky JL (2008) Dissecting the ER-associated degradation of a misfolded polytopic membrane protein. *Cell* 132:101–112.
37. Otto H, *et al.* (2005) The chaperones MPP11 and Hsp70L1 form the mammalian ribosome-associated complex. *Proc Natl Acad Sci USA* 102:10064–10069.
38. Hundley H, *et al.* (2002) The *in vivo* function of the ribosome-associated Hsp70, Ssz1, does not require its putative peptide-binding domain. *Proc Natl Acad Sci USA* 99:4203–4208.

CELL BIOLOGY